PERGAMON

Engineering Fracture Mechanics 69 (2002) 1769–1790

Engineering Fracture Mechanics

www.elsevier.com/locate/engfracmech

A viscoelastic functionally graded strip containing a crack subjected to in-plane loading

Z.-H. Jin, Glaucio H. Paulino *

Department of Civil and Environmental Engineering, Newmark Laboratory, University of Illinois at Urbana-Champaign, 205 North Mathews Avenue, Urbana, IL 61801, USA

Received 20 October 2000; received in revised form 13 April 2001; accepted 17 April 2001

Abstract

In this paper, a crack in a viscoelastic strip of a functionally graded material (FGM) is studied under tensile loading conditions. The extensional relaxation modulus is assumed as $E = E_0 \exp(\beta y/h) f(t)$, where h is a scale length and $f(t)$ is a nondimensional function of time t either having the form $f(t) = E_\infty/E_0 + (1 - E_\infty/E_0)\exp(-t/t_0)$ for a linear standard solid or $f(t) = (t_0/t)^q$ for a power law material model, where E_0, E_∞, β, t_0 and q are material constants. An extensional relaxation function in the form $E = E_0 \exp(\beta y/h)[t_0 \exp(\delta y/h)/t]^q$ is also considered, in which the relaxation time depends on the Cartesian coordinate y exponentially with δ being a material constant describing the gradation of the relaxation time. The Poisson's ratio is assumed to have the form $v = v_0(1 + \gamma y/h)\exp(\beta y/h)g(t)$, where v_0 and γ are material constants, and $g(t)$ is a nondimensional function of time t. An elastic FGM crack problem is first solved and the "correspondence principle" is used to obtain both mode I and mode II stress intensity factors, and the crack opening/sliding displacements for the viscoelastic FGM considering various material models.

Keywords: Crack; Stress intensity factor; Viscoelasticity; Standard linear solid; Power law material; Functionally graded material

1. Introduction

Materials exhibit creep and relaxation behavior at elevated temperatures. Upon such conditions, deformation creep occurs under constant stress state, while stress relaxation takes place under constant strain state. In the framework of linear continuum theory, such behavior can be studied by viscoelasticity. Generally speaking, the viscoelastic response may be obtained from the elastic solution via the *correspondence principle* [1], or the analogy between the Laplace transform of the viscoelastic solution and the corresponding elastic solution. Fracture behavior of homogeneous materials has been investigated by Broberg [2] who has given some examples of stress intensity factors (SIFs) for stationary cracks in viscoelastic solids. Atkinson and Chen [3,4] have investigated cracks in layered viscoelastic materials. Crack growth problems have been studied, for example, by Knauss [5] and Shapery [6–8].

* Corresponding author. Fax: +1-217-265-8041.
E-mail address: paulino@uiuc.edu (G.H. Paulino).

0013-7944/02/$ - see front matter © 2002 Elsevier Science Ltd. All rights reserved.
PII: S0013-7944(02)00049-8

Functionally graded materials (FGMs) are an alternative to homogeneous materials or layered composites, and are promising candidates for future advanced technological applications [9,10]. The material properties of FGMs are continuously graded with gradual change in *microstructural details* over predetermined geometrical orientations and distances, such as composition, morphology, and crystal structure [11,12]. In applications involving severe thermal gradients (e.g. thermal protection systems), FGM systems take advantage of heat and corrosion resistance typical of ceramics, and mechanical strength and toughness typical of metals. Several aspects of fracture mechanics of FGMs have been studied, for example, basic theory and review [13], crack tip fields [14,15], crack growth resistance curve [16], crack deflection [17], conservation laws [18], strain gradient theory [19], fracture testing [20], and statistical models [21].

Under elevated temperature conditions, FGMs also exhibit creep and relaxation behavior. For polymer-based FGMs (see, for example, [22–24]), their creep and relaxation behavior may be studied by viscoelasticity. However, in general, the correspondence principle, does not hold for FGMs. To avoid this problem, Paulino and Jin [25] have shown that the correspondence principle can still be used to obtain the viscoelastic solution *for a class of FGMs exhibiting relaxation* (*or creep*) *functions with separable kernels in space and time*. By using such *revisited correspondence principle* for FGMs, they have subsequently studied crack problems of FGM strips subjected to antiplane shear conditions [26,27]. Other studies on crack problems of nonhomogeneous viscoelastic materials directly solve the viscoelastic governing equations. For example, Schovanec and co-workers have considered stationary cracks [28], quasi-static crack propagation [29] and dynamic crack propagation [30] in nonhomogeneous viscoelastic media under antiplane shear conditions. Schovanec and Walton also considered quasi-static propagation of a plane strain mode I crack in a power-law inhomogeneous linearly viscoelastic body [31] and calculated the corresponding energy release rate [32]. Although a separable form for the relaxation functions was employed in Refs. [28–32], no use of the correspondence principle was made. Recently, Yang [33] performed stress analysis in FGM cylinders where steady-state creep conditions are considered only for the homogeneous material.

In the present study, a stationary crack in a viscoelastic FGM strip is investigated under tensile loading conditions. The extensional relaxation function of the material is assumed as

$$E = E_0 \exp(\beta y/h) f(t),$$

where h is a scale length and $f(t)$ is a nondimensional function of time t either having the form

$$f(t) = E_\infty/E_0 + (1 - E_\infty/E_0)\exp(-t/t_0): \quad \text{linear standard solid}$$

or

$$f(t) = (t_0/t)^q: \quad \text{power law material.}$$

We also consider the following variant form of the power law material model

$$E = E_0 \exp(\beta y/h)[t_0 \exp(\delta y/h)/t]^q,$$

in which *the relaxation time depends on y exponentially.* In the above expressions, the parameters E_0, E_∞, β, t_0; δ, q are material constants. The Poisson's ratio is assumed to take the form (also separable in space and time)

$$v = v_0(1 + \gamma y/h)\exp(\beta y/h) g(t).$$

where v_0 and γ are material constants, and $g(t)$ is a nondimensional function of time t. The material models considered above may be suitable, for example, for two phase polymeric/polymeric FGMs with their basic constitutents having different Young's moduli and Poisson's ratios but having approximately the same viscoelastic relaxation behavior. Since an FGM is a special composite of its constitutents, the viscoelastic relaxation behavior may remain unchanged if its constitutents have the same relaxation behavior. Thus, the

relaxation moduli of the FGM would have separable forms in space and time. Further, the independent material constants β and γ describe the spatial gradation in Young's modulus and Poisson's ratio.

According to the correspondence principle, we first consider a crack in an elastic strip of an FGM with the following properties:

$$E = E_0 \exp(\beta y/h), \quad v = v_0(1 + \gamma y/h)\exp(\beta y/h).$$

The Laplace transform of the viscoelastic solution is directly obtained from the elastic solution. For the traction boundary value problem, the stress intensity factors are the same as those for the nonhomogeneous elastic strip. The crack opening/sliding displacements, however, are functions of time.

The remainder of this paper is organized as follows. The basic equations of viscoelasticity are provided in the next section and some viscoelastic constitutive models for FGMs are discussed in Section 3. The boundary value problem of a crack in a viscoelastic FGM strip is presented in Section 4. SIFs and crack opening/sliding displacements are discussed in Sections 5 and 6, respectively. Relevant numerical aspects for solving the governing system of integral equations are given in Section 7. Numerical results of SIFs and crack opening/sliding displacements are given in Section 8. Finally, some concluding remarks and extensions are given in Section 9. Appendix A, containing the explicit form of the Fredholm kernels in the integral equations, supplements the paper.

2. Basic equations

The basic equations of quasi-static viscoelasticity of FGMs are the equilibrium equation (in the absence of body forces)

$$\sigma_{ij,j} = 0, \tag{1}$$

the strain–displacement relationship

$$\varepsilon_{ij} = \tfrac{1}{2}(u_{i,j} + u_{j,i}), \tag{2}$$

and the viscoelastic constitutive law

$$e_{ij} = \int_0^t J_1(\boldsymbol{x}, t-\tau)\frac{\mathrm{d}s_{ij}}{\mathrm{d}\tau}\mathrm{d}\tau, \quad \varepsilon_{kk} = \int_0^t J_2(\boldsymbol{x}, t-\tau)\frac{\mathrm{d}\sigma_{kk}}{\mathrm{d}\tau}\mathrm{d}\tau \tag{3}$$

with

$$s_{ij} = \sigma_{ij} - \frac{1}{3}\sigma_{kk}\delta_{ij}, \quad e_{ij} = \varepsilon_{ij} - \frac{1}{3}\varepsilon_{kk}\delta_{ij}, \tag{4}$$

where σ_{ij} are stresses, ε_{ij} are strains, s_{ij} and e_{ij} are deviatoric components of the stress and strain tensors, respectively, u_i are displacements, δ_{ij} is the Kronecker delta, $\boldsymbol{x} = (x_1, x_2, x_3)$, $J_1(\boldsymbol{x}, t)$ and $J_2(\boldsymbol{x}, t)$ are the creep functions, t denotes time, and the Latin indices have the range 1–3 with repeated indices implying the summation convention. Note that *for FGMs the creep functions also depend on spatial positions*, whereas in homogeneous viscoelasticity, they are only functions of time, i.e. $J_1 \equiv J_1(t)$ and $J_2 \equiv J_2(t)$ [1].

The creep functions $J_1(\boldsymbol{x}, t)$ and $J_2(\boldsymbol{x}, t)$ are related to the relaxation function in extension, $E(\boldsymbol{x}, t)$, and the relaxation function in Poisson's ratio, $v(\boldsymbol{x}, t)$, by the following equations [1]:

$$\overline{J}_1 = \frac{1 + p\bar{v}}{p^2\overline{E}}, \quad \overline{J}_2 = \frac{1 - 2p\bar{v}}{p^2\overline{E}}, \tag{5}$$

where a bar over a variable means the Laplace transform, and p is the Laplace transform variable.

Under plane stress conditions, the Laplace transforms of the basic equations (1)–(3) are reduced to

$$\frac{\partial \bar{\sigma}_{xx}}{\partial x}+\frac{\partial \bar{\sigma}_{xy}}{\partial y}=0, \quad \frac{\partial \bar{\sigma}_{xy}}{\partial x}+\frac{\partial \bar{\sigma}_{yy}}{\partial y}=0, \tag{6}$$

$$\bar{\epsilon}_{xx}=\frac{\partial \bar{u}}{\partial x}, \quad \bar{\epsilon}_{yy}=\frac{\partial \bar{v}}{\partial y}, \quad \bar{\epsilon}_{xy}=\frac{1}{2}\left(\frac{\partial \bar{u}}{\partial y}+\frac{\partial \bar{v}}{\partial x}\right), \tag{7}$$

$$\bar{\epsilon}_{xx}=\frac{1}{p\bar{\bar{E}}}\left(\bar{\sigma}_{xx}-p\bar{\nu}\bar{\sigma}_{yy}\right), \quad \bar{\epsilon}_{yy}=\frac{1}{p\bar{\bar{E}}}\left(\bar{\sigma}_{yy}-p\bar{\nu}\bar{\sigma}_{xx}\right), \quad \bar{\epsilon}_{xy}=\frac{2(1+p\bar{\nu})}{p\bar{\bar{E}}}\bar{\sigma}_{xy}, \tag{8}$$

where $x \equiv x_1$, $y \equiv x_2$, and u and v are displacements in the x and y directions, respectively.

3. Viscoelastic models for FGMs

This section describes three viscoelastic material models considered in this investigation. The first is a *standard linear solid* with constant relaxation time

$$E=E_0\exp(\beta y/h)\left[\frac{E_\infty}{E_0}+\left(1-\frac{E_\infty}{E_0}\right)\exp\left(-\frac{t}{t_0}\right)\right], \tag{9}$$

where β, E_0, E_∞ and t_0 are material constants and h is a scale length (e.g., the strip thickness). The second model is a *power law material* with *constant relaxation time*

$$E=E_0\exp(\beta y/h)\left(\frac{t_0}{t}\right)^q, \quad 0<q<1, \tag{10}$$

where q is a material constant. The third model is still a power law material, but with *position-dependent relaxation time*

$$E=E_0\exp(\beta y/h)\left[\frac{t_0\exp(\delta y/h)}{t}\right]^q=E_0\exp[(\beta+\delta q)y/h]\left(\frac{t_0}{t}\right)^q, \tag{11}$$

where δ is a material constant. For all three models, the Poisson's ratio is assumed as

$$\nu=\nu_0(1+\gamma y/h)\exp(\beta y/h)g(t), \tag{12}$$

where ν_0 and γ are material constants, and $g(t)$ is a nondimensional function of time t. The spatial position dependent part of the Possion ratio (12) was first proposed by Delale and Erdogan [34] to study non-homogeneous elastic crack problems. Noda and Jin [35] later used it to investigate thermal crack problems in nonhomogeneous solids. The Poisson's ratio given by Eq. (12) is subjected to the condition that $-1 \leq \nu \leq 0.5$ [36].

With the assumptions (9)–(12) on the relaxation modulus and the Poisson's ratio, the correspondence principle for viscoelastic FGMs [25] can be used to study crack problems, i.e. *the Laplace transformed viscoelastic FGM solution can be obtained directly from the solution of the corresponding elastic FGM solution by replacing E_0 and ν_0 with $pE_0\bar{f}(p)$ and $p\nu_0\bar{g}(p)$, respectively. The final solution is realized upon inverting the transformed solution*, where $\bar{f}(p)$ and $\bar{g}(p)$ are the Laplace transforms of $f(t)$ and $g(t)$, respectively. For the *standard linear solid* (9), $f(t)$ is given by

$$f(t)=\left[\frac{E_\infty}{E_0}+\left(1-\frac{E_\infty}{E_0}\right)\exp\left(-\frac{t}{t_0}\right)\right]. \tag{13}$$

For the *power law material* (10) or (11), $f(t)$ is

$$f(t) = \left(\frac{t_0}{t}\right)^q. \tag{14}$$

Since the function $g(t)$ does not affect the final governing equations and boundary conditions considered (see Section 4), no specific functional form is required.

It can be clearly seen from (9) to (12) that the relaxation moduli and the Poisson's ratio are separable functions in space and time. This is a necessary condition for applying the *revisited correspondence principle* [25]. This kind of relaxation functions may be appropriate for an FGM with its constituent materials having different Young's moduli and Poisson's ratios but having approximately the same viscoelastic relaxation behavior. Since the FGM is a special composite of its constitutents, the viscoelastic relaxation behavior may remain unchanged if its constitutents have the same relaxation behavior. Thus, the relaxation moduli of the FGM would have separable forms in space and time. Further, the material constants β and γ describe the spatial gradation in Young's modulus and Poisson's ratio. For model (9), the separable form of the extensional relaxation modulus means that the constituents should have the same ratio E_∞/E_0 and relaxation time t_0. For model (10), this implies that the constituents should have the same relaxation time t_0 and parameter q. For model (11), however, it is only required that the constituents have the same parameter q. The constituents may have different relaxation times. Potentially, this kind of FGMs may include some polymeric/polymeric materials such as propylene-homopolymer/Acetal-copolymer. The relaxation behavior of propylene homopolymer and Acetal copolymer are found to be similar—see Figs. 7.5 and 10.3, respectively, of Ogorkiewicz [37].

4. A crack in a viscoelastic FGM strip

Consider an infinite nonhomogeneous viscoelastic strip containing a crack of length $2a$, as shown in Fig. 1. The strip is subjected to a uniform tension $\sigma_0\Sigma(t)$ in the y-direction along both the lower boundary ($y = -h_1$) and the upper boundary ($y = h_2$), where σ_0 is a constant and $\Sigma(t)$ is a nondimensional function of time t. It is assumed that the crack lies on the x-axis, from $-a$ to a. The crack surfaces remain traction free. The boundary conditions of the crack problem, therefore, are

$$\sigma_{xy} = 0, \quad \sigma_{yy} = \sigma_0\Sigma(t), \quad y = -h_1, \quad |x| < \infty, \tag{15}$$

$$\sigma_{xy} = 0, \quad \sigma_{yy} = \sigma_0\Sigma(t), \quad y = h_2, \quad |x| < \infty, \tag{16}$$

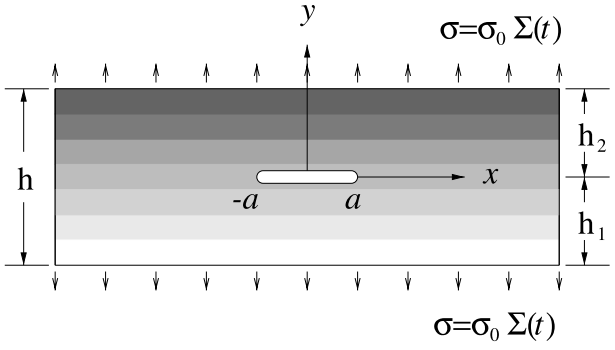

Fig. 1. A viscoelastic FGM strip occupying the region $|x| < \infty$ and $-h_1 \leqslant y \leqslant h_2$ with a crack at $|x| \leqslant a$ and $y = 0$. The boundaries of the strip ($y = -h_1, h_2$) are subjected to uniform traction $\sigma_0\Sigma(t)$.

$$\sigma_{xy} = \sigma_{yy} = 0, \quad y = 0, \quad |x| \leq a, \tag{17}$$

$$\sigma_{xy}(x, 0^+) = \sigma_{xy}(x, 0^-), \quad a < |x| < \infty, \tag{18}$$

$$\sigma_{yy}(x, 0^+) = \sigma_{yy}(x, 0^-), \quad a < |x| < \infty, \tag{19}$$

$$u(x, 0^+) = u(x, 0^-), \quad a < |x| < \infty, \tag{20}$$

$$v(x, 0^+) = v(x, 0^-), \quad a < |x| < \infty. \tag{21}$$

According to the correspondence principle described in Ref. [25] and the previous section, one can first consider a nonhomogeneous elastic material with Young's modulus and Poisson's ratio

$$E = E_0 \exp(\beta y/h), \quad v = v_0(1 + \gamma y/h) \exp(\beta y/h), \tag{22}$$

respectively, and the viscoelastic solutions for models (9) and (10) may be obtained by the correspondence principle. Note that for material model (11) the viscoelastic solution can still be obtained by the correspondence principle provided that the corresponding elastic material has the following Young's modulus and Poisson's ratio:

$$E = E_0 \exp[(\beta + q\delta)y/h], \quad v = v_0(1 + \gamma y/h) \exp[(\beta + q\delta)y/h]. \tag{23}$$

For the elastic crack problem, the solution consists of a regular solution (for an uncracked strip) and a purturbed solution by the crack. The stresses for the regular solution are

$$\sigma_{xx} = v(y)\sigma_0\Sigma(t) + E(y)(C_1 y + C_2), \tag{24}$$

$$\sigma_{yy} = \sigma_0\Sigma(t), \tag{25}$$

$$\sigma_{xy} = 0, \tag{26}$$

where C_1 and C_2 are constants which can be determined by the displacement constraint conditions. These constants do not influence the final stress intensity factor and crack opening/sliding displacement results.

For the perturbed problem by the crack, the following boundary conditions need to be satisfied

$$\sigma_{xy} = 0, \quad \sigma_{yy} = 0, \quad y = -h_1, \quad |x| < \infty, \tag{27}$$

$$\sigma_{xy} = 0, \quad \sigma_{yy} = 0, \quad y = h_2, \quad |x| < \infty, \tag{28}$$

$$\sigma_{xy} = 0, \quad y = 0, \quad |x| \leqslant a, \tag{29}$$

$$\sigma_{yy} = -\sigma_0\Sigma(t), \quad y = 0, \quad |x| \leqslant a, \tag{30}$$

$$\sigma_{xy}(x, 0^+) = \sigma_{xy}(x, 0^-), \quad a < |x| < \infty, \tag{31}$$

$$\sigma_{yy}(x, 0^+) = \sigma_{yy}(x, 0^-), \quad a < |x| < \infty, \tag{32}$$

$$u(x, 0^+) = u(x, 0^-), \quad a < |x| < \infty, \tag{33}$$

$$v(x, 0^+) = v(x, 0^-), \quad a < |x| < \infty. \tag{34}$$

The governing differential equation in terms of the Airy stress function $\Phi(x, y)$ for the nonhomogeneous elastic material (22) is [34]

$$\nabla^2\nabla^2\Phi - 2\left(\frac{\beta}{h}\right)\frac{\partial(\nabla^2\Phi)}{\partial y} + \left(\frac{\beta}{h}\right)^2\frac{\partial^2\Phi}{\partial y^2} = 0. \tag{35}$$

The stresses can be expressed in terms of Φ as

$$\sigma_{xx} = \frac{\partial^2\Phi}{\partial y^2}, \quad \sigma_{yy} = \frac{\partial^2\Phi}{\partial x^2}, \quad \sigma_{xy} = -\frac{\partial^2\Phi}{\partial x\partial y}. \tag{36}$$

The displacements are related to Φ by the constitutive relationship

$$\frac{\partial u}{\partial x} = \frac{1}{E_0}\left[\exp(-\beta y/h)\sigma_{xx} - \nu_0(1+\gamma y/h)\sigma_{yy}\right], \tag{37}$$

$$\frac{\partial v}{\partial y} = \frac{1}{E_0}\left[\exp(-\beta y/h)\sigma_{yy} - \nu_0(1+\gamma y/h)\sigma_{xx}\right], \tag{38}$$

$$\frac{\partial u}{\partial y} + \frac{\partial v}{\partial x} = \frac{2[\exp(-\beta y/h) + \nu_0(1+\gamma y/h)]}{E_0}\sigma_{xy}. \tag{39}$$

By using the Fourier transform method (see, for example, Ref. [38]), the boundary value problem described by Eqs. (27)–(39) can be reduced to the following system of singular integral equations:

$$\begin{aligned}
&\int_{-1}^{1}\left[\frac{\varphi_1(s)}{s-r} + k_{11}(r,s,\beta)\varphi_1(s) + k_{12}(r,s,\beta)\varphi_2(s)\right]\mathrm{d}s = 0, \quad |r| \leqslant 1,\\
&\int_{-1}^{1}\left[\frac{\varphi_2(s)}{s-r} + k_{21}(r,s,\beta)\varphi_1(s) + k_{22}(r,s,\beta)\varphi_2(s)\right]\mathrm{d}s = -2\pi\frac{\sigma_0\Sigma(t)}{E_0}, \quad |r| \leqslant 1,
\end{aligned} \tag{40}$$

where the unknown density functions $\varphi_1(r)$ and $\varphi_2(r)$ are defined by

$$\begin{aligned}
\varphi_1(x) &= \frac{\partial}{\partial x}[u(x,0^+) - u(x,0^-)],\\
\varphi_2(x) &= \frac{\partial}{\partial x}[v(x,0^+) - v(x,0^-)],
\end{aligned} \tag{41}$$

the nondimensional coordinate r is

$$r = x/a, \tag{42}$$

and the Fredholm kernels $k_{ij}(r,s,\beta)$ $(i,j = 1, 2)$ can be found in Ref. [35] and are compiled in the Appendix A for completeness.

The functions $\varphi_1(r)$ and $\varphi_2(r)$ satisfy the following uniqueness condition

$$\int_{-1}^{1}\varphi_i(r)\mathrm{d}r = 0, \quad (i = 1,2), \tag{43}$$

They can be further expressed as

$$\varphi_i(r) = \psi_i(r)/\sqrt{1-r^2}, \quad (i = 1,2), \tag{44}$$

where $\psi_i(r)$ $(i = 1, 2)$ are continuous for $r \in [-1, 1]$. When $\varphi_i(r)$ are normalized by $\sigma_0\Sigma(t)/E_0$, the elastic Mode I and mode II SIFs, K_{I}^e and K_{II}^e, are obtained as

$$\begin{aligned}
K_{\mathrm{I}}^e &= -\tfrac{1}{2}\psi_2(1,\beta)\sigma_0\Sigma(t)\sqrt{\pi a},\\
K_{\mathrm{II}}^e &= -\tfrac{1}{2}\psi_1(1,\beta)\sigma_0\Sigma(t)\sqrt{\pi a}.
\end{aligned} \tag{45}$$

Here, the notation $\psi_i(1,\beta)$ $(i=1,2)$ is adopted to emphasize the dependence of $\psi_1(1)$ and $\psi_2(1)$ on the material parameter β.

5. Stress intensity factors

The SIFs for the viscoelastic FGMs (9)–(11) with the Poisson ratio (12) can be obtained by using the correspondence principle between the elastic and the Laplace transformed viscoelastic equations. Since no other material parameters appear in the SIFs (45), except for the nondimensional parameter β, the SIFs for the viscoelastic FGMs are also given by Eq. (45) by means of the correspondence principle, i.e.

$$K_{\mathrm{I}} = -\tfrac{1}{2}\psi_2(1,\beta)\sigma_0\Sigma(t)\sqrt{\pi a} = K_{\mathrm{I}}^e,$$
$$K_{\mathrm{II}} = -\tfrac{1}{2}\psi_1(1,\beta)\sigma_0\Sigma(t)\sqrt{\pi a} = K_{\mathrm{II}}^e.$$

For the *power law material with position-dependent relaxation time* (11), the SIFs are

$$\begin{aligned} K_{\mathrm{I}} &= -\tfrac{1}{2}\psi_2(1,\beta+q\delta)\sigma_0\Sigma(t)\sqrt{\pi a},\\ K_{\mathrm{II}} &= -\tfrac{1}{2}\psi_1(1,\beta+q\delta)\sigma_0\Sigma(t)\sqrt{\pi a}. \end{aligned} \tag{46}$$

It is seen that q and δ (parameters describing the position dependence of the relaxation time) affect the SIFs only through the combined parameter $(\beta+q\delta)$.

6. Crack opening/sliding displacements

Crack opening/sliding displacements are important parameters in assessing fracture behavior. For the crack problem considered here, those displacements will also evolve with time. Thus, the crack opening/sliding displacements are first given for general time-dependent loading by using the correspondence principle. Two special loading conditions, i.e. Heaviside step loading and exponential loading are subsequently considered.

It follows from Eqs. (41) and (44), and the correspondence principle, that the Laplace transforms of the crack opening/sliding displacements under time-dependent loading, $\sigma_0\Sigma(t)$, can be expressed by the density functions $\varphi_1(x)$ and $\varphi_2(x)$, or $\psi_1(r)$ and $\psi_2(r)$ (normalized by $\sigma_0\Sigma(t)/E_0$), as follows:

$$\begin{aligned} \bar{[u]} &= \bar{u}(x,0^+) - \bar{u}(x,0^-) = \frac{\sigma_0\bar{\Sigma}(p)}{pE_0\bar{f}(p)}\int_{-a}^{x}\varphi_1(x')\mathrm{d}x' = \frac{a\sigma_0\bar{\Sigma}(p)}{pE_0\bar{f}(p)}\int_{-1}^{r}\frac{\psi_1(s)}{\sqrt{1-s^2}}\mathrm{d}s,\\ \bar{[v]} &= \bar{v}(x,0^+) - \bar{v}(x,0^-) = \frac{\sigma_0\bar{\Sigma}(p)}{pE_0\bar{f}(p)}\int_{-a}^{x}\varphi_2(x')\mathrm{d}x' = \frac{a\sigma_0\bar{\Sigma}(p)}{pE_0\bar{f}(p)}\int_{-1}^{r}\frac{\psi_2(s)}{\sqrt{1-s^2}}\mathrm{d}s, \end{aligned} \tag{47}$$

where $\bar{\Sigma}(p)$ is the Laplace transform of $\Sigma(t)$ and $\bar{f}(p)$ is the Laplace transform of $f(t)$ which is given in Eqs. (13) and (14).

The crack opening/sliding displacements are then obtained as follows:

$$\begin{aligned} [u] &= u(x,0^+) - u(x,0^-) = \left(\frac{a\sigma_0}{E_0}\right)F(t)\int_{-1}^{r}\frac{\psi_1(s)}{\sqrt{1-s^2}}\mathrm{d}s,\\ [v] &= v(x,0^+) - v(x,0^-) = \left(\frac{a\sigma_0}{E_0}\right)F(t)\int_{-1}^{r}\frac{\psi_2(s)}{\sqrt{1-s^2}}\mathrm{d}s, \end{aligned} \tag{48}$$

where

$$F(t) = \mathscr{L}^{-1}\left[\frac{\overline{\Sigma}(p)}{p\bar{f}(p)}\right], \tag{49}$$

in which $\mathscr{L}^{-1}$ represents the inverse Laplace transform.

6.1. Heaviside step loading

For the Heaviside step loading,

$$\Sigma(t) = H(t) \rightarrow \overline{\Sigma}(p) = 1/p, \tag{50}$$

where $H(t)$ is the Heaviside step function. Thus the function $F(t)$ in Eqs. (48) and (49) becomes

$$F(t) = \frac{E_0}{E_\infty} - \left(\frac{E_0}{E_\infty} - 1\right)\exp\left(-\frac{E_\infty t}{E_0 t_0}\right), \tag{51}$$

for the *standard linear solid*, and

$$F(t) = \frac{(t/t_0)^q}{\Gamma(1-q)\Gamma(1+q)}, \tag{52}$$

for the *power law material*, where $\Gamma(\cdot)$ is the Gamma function.

6.2. Exponential loading

Now consider the exponential loading [2] as another example

$$\Sigma(t) = \exp(-t/t_L) \rightarrow \overline{\Sigma}(p) = 1/(p + 1/t_L), \tag{53}$$

where t_L is a positive constant (load relaxation time). The function $F(t)$ is then given by

$$F(t) = \frac{1}{E_\infty/E_0 - t_0/t_L}\left[\left(1 - \frac{t_0}{t_L}\right)\exp\left(-\frac{t}{t_L}\right) - \left(1 - \frac{E_\infty}{E_0}\right)\exp\left(-\frac{E_\infty t}{E_0 t_0}\right)\right] \tag{54}$$

for the *standard linear solid*, and

$$F(t) = \frac{1}{\Gamma(1-q)\Gamma(q)t_0}\int_0^t \left(\frac{\tau}{t_0}\right)^{q-1}\exp\left(-\frac{t-\tau}{t_L}\right)\mathrm{d}\tau, \tag{55}$$

for the *power law material*.

7. Numerical solution of the governing system of integral equations

To obtain the numerical solution of the system of governing integral equations (40), the density functions, $\psi_i(r)$ $(i = 1, 2)$, are expanded into series of Chebyshev polynomials of the first kind. By noting the symmetric properties of the density functions (41), $\varphi_i(r)$ $(i = 1, 2)$, they are expressed as follows:

$$\begin{aligned}
\varphi_1(r) &= \frac{1}{\sqrt{1-r^2}}\sum_{n=1}^{\infty} b_n T_{2n}(r), \quad |r| \leqslant 1, \\
\varphi_2(r) &= \frac{1}{\sqrt{1-r^2}}\sum_{n=1}^{\infty} a_n T_{2n-1}(r), \quad |r| \leqslant 1,
\end{aligned} \tag{56}$$

where $T_n(r)$ are Chebyshev polynomials of the first kind, and a_n and b_n are unknown constants. It is noted that $\varphi_i(r)$ given by Eq. (56) already satisfy the condition (43).

By substituting the above equations into integral equation (40), we have

$$\begin{aligned}
&\sum_{n=1}^{\infty}\left\{\pi U_{2n-1}(r)a_n + H_n^{11}(r)a_n + H_n^{12}(r)b_n\right\} = 0, \quad |r| \leqslant 1,\\
&\sum_{n=1}^{\infty}\left\{\pi U_{2n-2}(r)b_n + H_n^{21}(r)a_n + H_n^{22}(r)b_n\right\} = -2\pi\frac{\sigma_0\Sigma(t)}{E_0}, \quad |r| \leqslant 1,
\end{aligned} \tag{57}$$

where $U_n(r)$ are Chebyshev polynomials of the second kind and $H_n^{ij}(r)$ $(i,j = 1, 2)$ are given by

$$\begin{aligned}
H_n^{11}(r) &= \int_{-1}^{1} k_{11}(r,s,\beta)\frac{T_{2n}(s)}{\sqrt{1-s^2}}\mathrm{d}s,\\
H_n^{12}(r) &= \int_{-1}^{1} k_{12}(r,s,\beta)\frac{T_{2n-1}(s)}{\sqrt{1-s^2}}\mathrm{d}s,\\
H_n^{21}(r) &= \int_{-1}^{1} k_{21}(r,s,\beta)\frac{T_{2n}(s)}{\sqrt{1-s^2}}\mathrm{d}s,\\
H_n^{22}(r) &= \int_{-1}^{1} k_{22}(r,s,\beta)\frac{T_{2n-1}(s)}{\sqrt{1-s^2}}\mathrm{d}s.
\end{aligned} \tag{58}$$

To solve the functional equations (57), the series on the left hand side are first truncated at the Nth term. A collocation technique [38] is then used and the collocation points, r_i, are chosen as the roots of the Chebyshev polynomials of the first kind

$$r_i = \cos\frac{(2i-1)\pi}{2N}, \quad i = 1,2,\ldots,N. \tag{59}$$

The functional equations (57) are then reduced to a linear algebraic equation system

$$\begin{aligned}
&\sum_{n=1}^{N}\left\{\pi U_{2n-1}(r_i)a_n + H_n^{11}(r_i)a_n + H_n^{12}(r_i)b_n\right\} = 0,\\
&\sum_{n=1}^{N}\left\{\pi U_{2n-2}(r_i)b_n + H_n^{21}(r_i)a_n + H_n^{22}(r_i)b_n\right\} = -2\pi\frac{\sigma_0\Sigma(t)}{E_0}, \quad i = 1,2,\ldots,N.
\end{aligned} \tag{60}$$

After a_n and b_n $(n = 1, 2, \ldots, N)$ are determined, the nondimensional SIFs, K_{I}^* and K_{II}^*, are computed as follows:

$$K_{\mathrm{I}}^* = -\frac{1}{2}\psi_2(1,\beta) = -\frac{1}{2}\sum_{n=1}^{N} b_n, \tag{61}$$

$$K_{\mathrm{II}}^* = -\frac{1}{2}\psi_1(1,\beta) = -\frac{1}{2}\sum_{n=1}^{N} a_n. \tag{62}$$

In the following numerical calculations, it is found that 20 collocation points lead to a convergent SIF result.

8. Numerical results

Numerical results for SIFs are first calculated for a homogeneous elastic strip with a central crack (see Fig. 1). Table 1 shows the SIFs of the present calculations and those reported in the handbook by Tada et al. [39]. It is seen from the table that the SIFs are in good agreement. Another example considered is a semi-infinite homogeneous plane with a sub-surface crack, which was studied by Erdogan et al. [38]. The geometry is modeled by a cracked strip with the ratio $h_1/h = 0.01$ in this study (see Fig. 1). The SIFs from the present calculations and Ref. [38] are listed in Table 2. Again, it is observed that the SIFs are in good agreement. It should be noted that the existing results in Refs. [38,39] are also approximate solutions.

Fig. 2 shows normalized SIFs (see (61) and (62)), K_{I}^{*} and K_{II}^{*}, versus the nondimensional crack length $2a/h$ considering various nonhomogeneous parameter β for the linear standard solid and the power law model with constant relaxation time (see Eqs. (9) and (10)). As noted in Section 5, the SIFs are identical for both models. The crack is located in the middle of the strip, i.e. $h_2 = 0.5h$. Fig. 2(a) is the result for the mode I SIF. It is seen that the mode I SIF increases with increasing ratio $2a/h$ for all β values considered here. The SIF is higher than that of the corresponding homogeneous material ($\beta = 0$). The mode I SIF is an even function of β. However, this symmetry is valid only for the crack located in the center of the strip. Fig. 2(b) shows the result of mode II SIF. The mode II SIF is asymmetric about $\beta = 0$ (again, this anti-symmetry is valid only for the crack located in the center of the strip). The absolute value of the mode II SIF increases with increasing $2a/h$. As expected, the mode II SIF is zero for this crack geometry for a homogeneous strip ($\beta = 0$).

For the crack problem considered here, the SIFs for the FGM are, in general, higher than those for the corresponding homogeneous material (see Fig. 2 and the following figures). The higher SIFs do not necessarily mean that the FGM is inferior to the homogeneous materials. In fact, ceramic/metal FGMs usually have higher fracture toughness than monolithic ceramics. Therefore they can withstand higher SIFs. For example, Jin and Batra [16] have theoretically predicted that an alumina/nickel FGM may have a fracture toughness up to 30 times higher than that of alumina.

Fig. 3(a) and (b) shows the SIF results for a crack located at a distance of $h_2 = 0.1h$ from the upper edge of the strip (see Fig. 1). It is seen from Fig. 3(a) that in general, the mode I SIF is not symmetric about $\beta = 0$. This is anticipated since the geometry is not symmetrical about the crack line. The mode I SIF for negative β is slightly larger than that for the corresponding positive β with the same absolute value. For

Table 1
Mode I SIFs for a homogeneous strip with a central crack

$2a/h$	SIF (this study)	SIF (Ref. [39])
0.1	1.01	1.01
0.67	1.42	1.42
1.0	1.82	1.88
2.0	3.29	3.42

Table 2
Modes I and II SIFs for a semi-infinite homogeneous plane with a sub-surface crack

$2a/h_1$	Mode I SIF (this study)	Model I SIF (Ref. [38])	Mode II SIF (this study)	Model II SIF (Ref. [38])
0.67	1.0779	1.0778	0.0124	0.0123
1.0	1.1633	1.1621	0.0368	0.0367
2.0	1.5111	1.4860	0.1849	0.1796

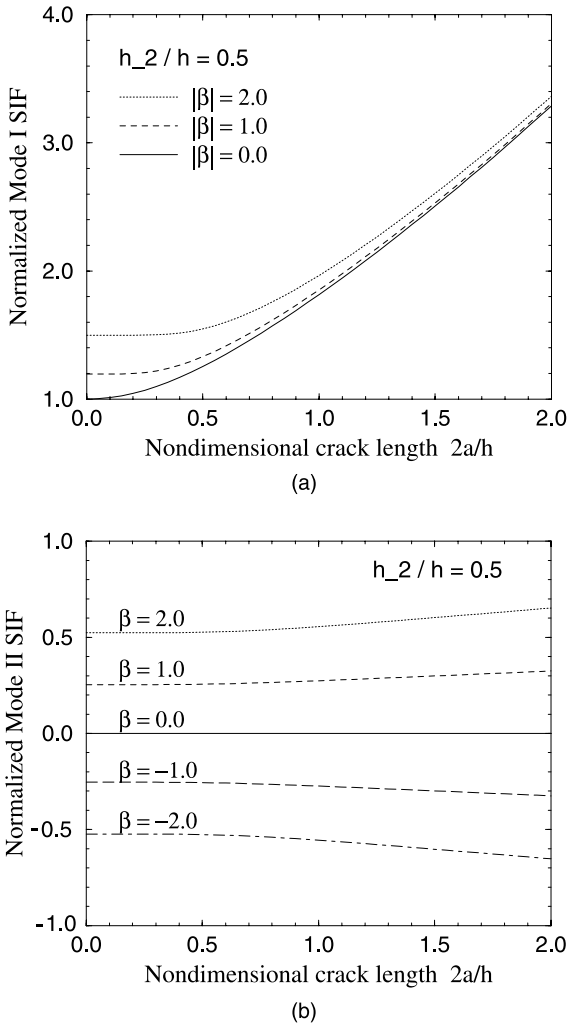

Fig. 2. Normalized SIFs versus nondimensional crack length, $2a/h$, for various material nonhomogeneous parameter β considering the linear standard solid and the power law material with constant relaxation time ($h_2 = 0.5h$), (a) mode I SIF; (b) mode II SIF.

very small nondimensional crack length $2a/h_2$, however, the mode I SIF is still approximately symmetric about $\beta = 0$. This is because the crack seems located in an infinite plate. It is observed from Fig. 3(b) that the magnitude of the mode II SIF increases with increasing $2a/h_2$ for $\beta < 0$. For $\beta > 0$, however, the magnitude of the mode II SIF may decrease or increase with increasing $2a/h_2$ depending on the value of β and the range of $2a/h_2$.

Fig. 4 shows normalized SIFs versus the nondimensional crack length $2a/h$ for $\beta = 2$ and various values of δ for the power law material with position-dependent relaxation time (see Eq. (11)). The crack is located in the middle of the strip. The effect of spatial position dependence of the relaxation time on the SIFs is reflected through the parameter δ. The parameter q is taken as 0.4 in all calculations. Thus the curves for $\delta = \pm 1$ may be obtained from the curve $\delta = 0$ by shifting this curve by $\beta = \mp 0.4$. It is clear from Fig. 4 that with respect to the corresponding model with constant relaxation time (i.e. $\delta = 0$), a positive δ increases SIFs when $\beta > 0$.

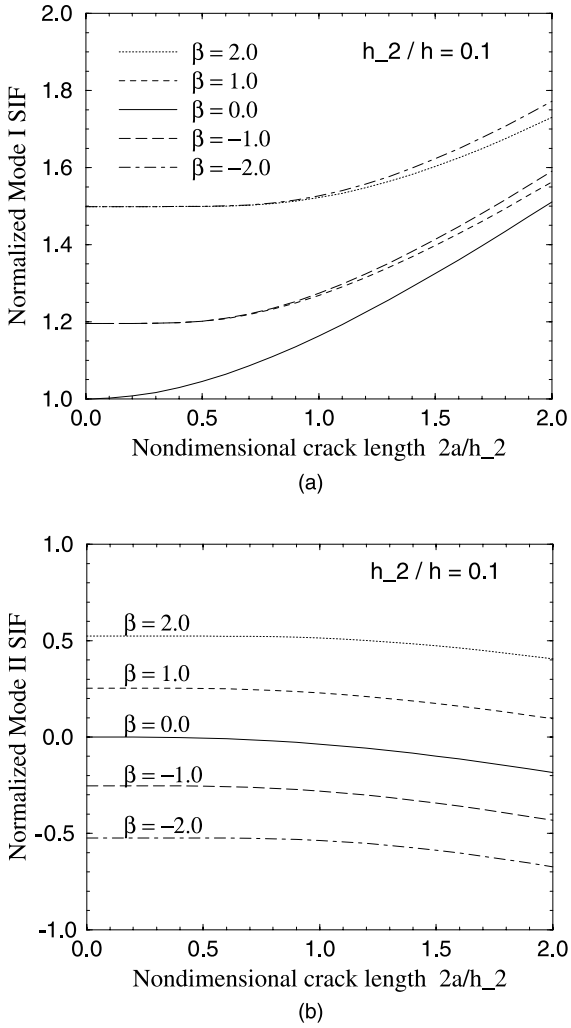

Fig. 3. Normalized SIFs versus nondimensional crack length, $2a/h_2$, for various material nonhomogeneous parameter β considering the linear standard solid and the power law material with constant relaxation time ($h_2 = 0.1h$), (a) mode I SIF; (b) mode II SIF.

Fig. 5 shows normalized SIFs versus the nondimensional crack length $2a/h$ for $\beta = -2$ and various values of δ for the power law material with position-dependent relaxation time (see Eq. (11)). The crack is located in the middle of the strip. In contrast with the result in Fig. 4, a negative δ increases the magnitudes of SIFs when $\beta < 0$.

Special attention needs to be paid when $|\beta|$ is relatively small compared with $|q\delta|$. In this case, the variation of SIFs with δ follows different paths depending on the value of $\beta + q\delta$. For example, Fig. 6 shows normalized SIFs versus the nondimensional crack length $2a/h$ for $\beta = 0.1$ and various values of δ for the power law material with position-dependent relaxation time (see Eq. (11)). The crack is again located in the middle of the strip. It is observed that the mode I SIF increases with an increase in the absolute value of δ (Fig. 6(a)). The magnitude of the mode II SIF also increases with an increase in the absolute value of δ (Fig. 6(b)).

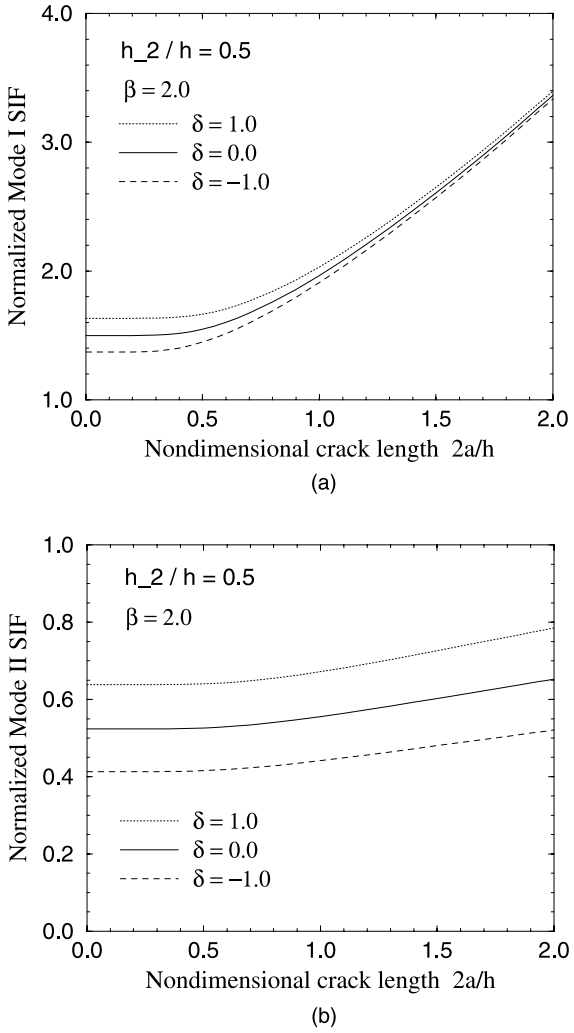

Fig. 4. Normalized SIFs versus nondimensional crack length, $2a/h$, for various material nonhomogeneous parameter δ considering the power law material with position-dependent relaxation time ($\beta = 2.0$, $q = 0.4$, $h_2 = 0.5h$), (a) mode I SIF; (b) mode II SIF.

Fig. 7 shows the SIF results for $\beta = 2$ and various values of δ for the power law material with position-dependent relaxation time (see Eq. (11)). The crack is located at a distance of $h_2 = 0.1h$ from the upper edge of the strip (see Fig. 1). The SIFs are found to follow a similar trend to that for a central crack except that the magnitude of mode II SIF decreases with increasing $2a/h_2$.

Fig. 8 shows the SIF results for $\beta = -2$ and various values of δ for the power law material with position-dependent relaxation time (see Eq. (11)). The crack is again located at a distance of $h_2 = 0.1h$ from the upper edge of the strip (see Fig. 1). The mixed mode SIFs follow a similar trend to that for a central crack (cf. Fig. 5).

Fig. 9(a) shows the crack opening displacement for the standard linear solid and the power law material with constant relaxation time (see Eq. (48)). The crack is located in the middle of the strip with $2a/h = 1$.

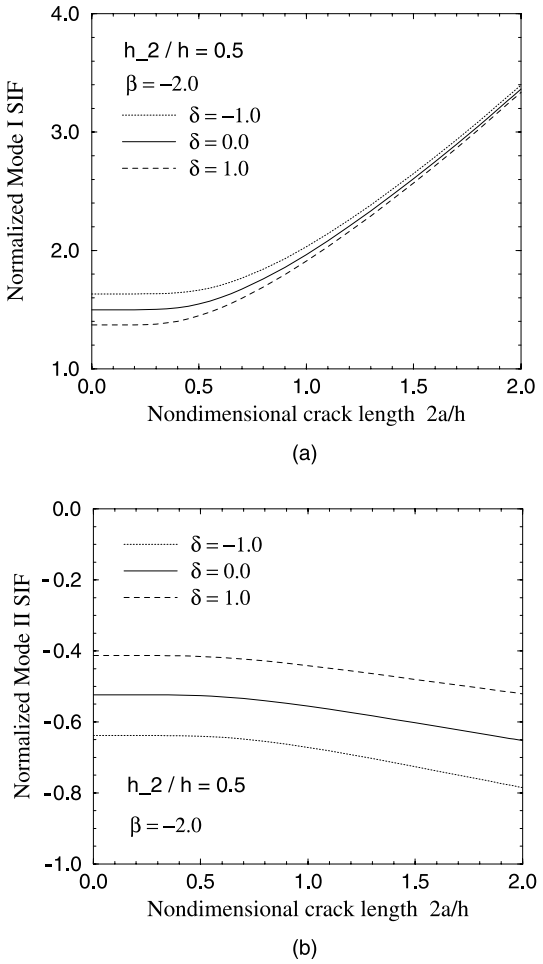

Fig. 5. Normalized SIFs versus nondimensional crack length, $2a/h$, for various material nonhomogeneous parameter δ considering the power law material with position-dependent relaxation time ($\beta = -2.0$, $q = 0.4$, $h_2 = 0.5h$), (a) mode I SIF; (b) mode II SIF.

For this special configuration, the crack opening displacement is symmetric about $\beta = 0$ (i.e. the same crack opening displacement is obtained for $\pm\beta$). It is seen from the figure that the crack opening displacement increases with increasing β. Fig. 9(b) depicts the crack sliding displacement for the same viscoelastic models. It is clear that the absolute value of the crack sliding displacement increases with increasing β. The crack sliding displacement vanishes for $\beta = 0$. This is anticipated because when the crack is located in the middle of a homogeneous strip, there is no mode II deformation.

Fig. 10 shows the crack opening/sliding displacements for a crack located in the middle of the strip of power law material with graded relaxation time. Three δ values are considered and β is taken as 2.0. As in the case of SIFs, with respect to the corresponding power law model with constant relaxation time (i.e. $\delta = 0$), a positive δ increases the crack opening displacement when $\beta > 0$. A negative δ would increase the crack opening displacement when $\beta < 0$, and increase the absolute value of the crack sliding displacement. This observation is consistent with the SIF investigation (see Fig. 4).

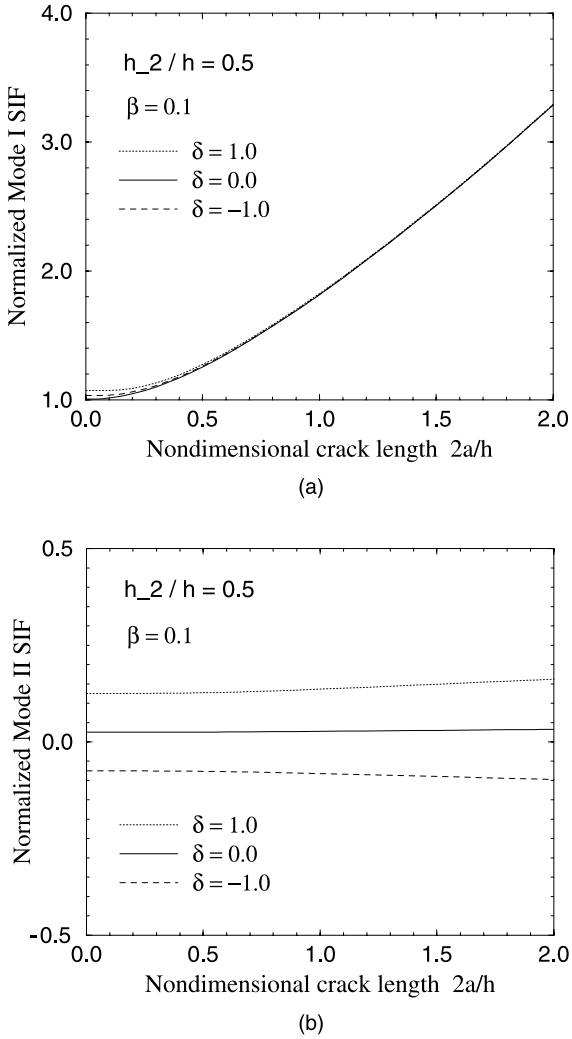

Fig. 6. Normalized SIFs versus nondimensional crack length, $2a/h$, for various material nonhomogeneous parameter δ considering the power law material with position-dependent relaxation time ($\beta = 0.1$, $q = 0.4$, $h_2 = 0.5h$), (a) mode I SIF; (b) mode II SIF.

9. Concluding remarks and extensions

The correspondence principle is used to study the SIFs and crack opening/sliding displacements for a crack in a viscoelastic FGM strip with relaxation functions having separable forms in space and time. Three viscoelastic models are considered, i.e. standard linear solid, power law material with constant relaxation time, and power law material with position-dependent relaxation time. Under traction boundary conditions, the SIFs for the models with constant relaxation times are the same as those for the corresponding nonhomogeneous elastic materials, while for the power law material with graded relaxation time, the SIFs are influenced by the gradation of the relaxation time. The crack opening/sliding displacements evolve with time reflecting the creep behavior of the material under traction boundary conditions.

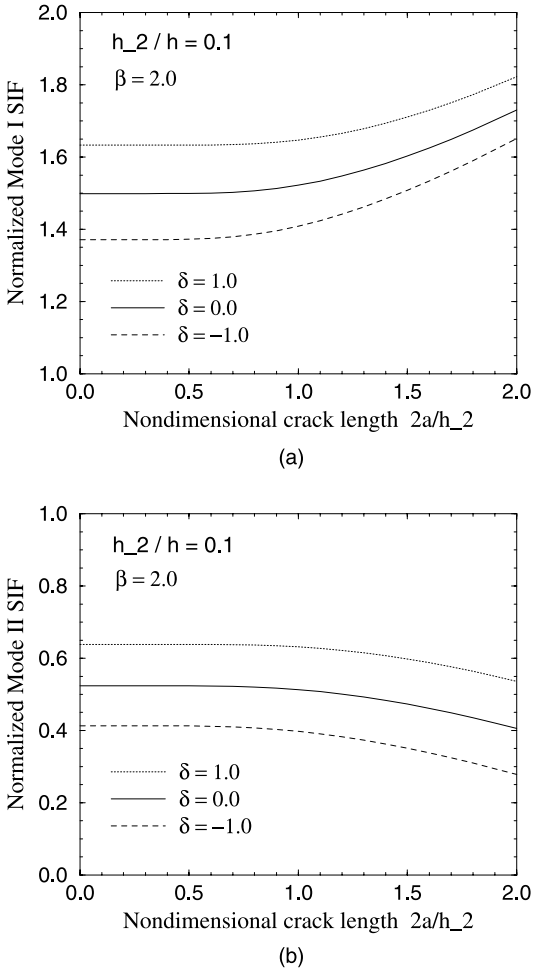

Fig. 7. Normalized SIFs versus nondimensional crack length, $2a/h_2$, for various material nonhomogeneous parameter δ considering the power law material with position-dependent relaxation time ($\beta = 2.0$, $h_2 = 0.1h$), (a) mode I SIF; (b) mode II SIF.

Natural extensions of this work include investigation of *displacement* (rather than traction) boundary conditions, *crack propagation*, and *experimental verification*. The solution of crack boundary value problems with displacement boundary conditions on the outer boundaries of the FGM strip may follow the methodology presented in this paper. The crack propagation modeling in viscoelastic FGMs can be thought as an extension of the techniques proposed by Wnuk [40], Knauss [5], and Shapery [6–8]. The experimental verification can be done by adapting the basic setup for fabricating large scale polymeric FGMs by Lambros et al. [23] to creep/relaxation and/or viscoelastic fracture testing. These topics are presently under consideration by the authors.

Acknowledgements

We would like to acknowledge the support from the National Science Foundation (NSF) under grant no. CMS-9996378 (Mechanics and Materials Program).

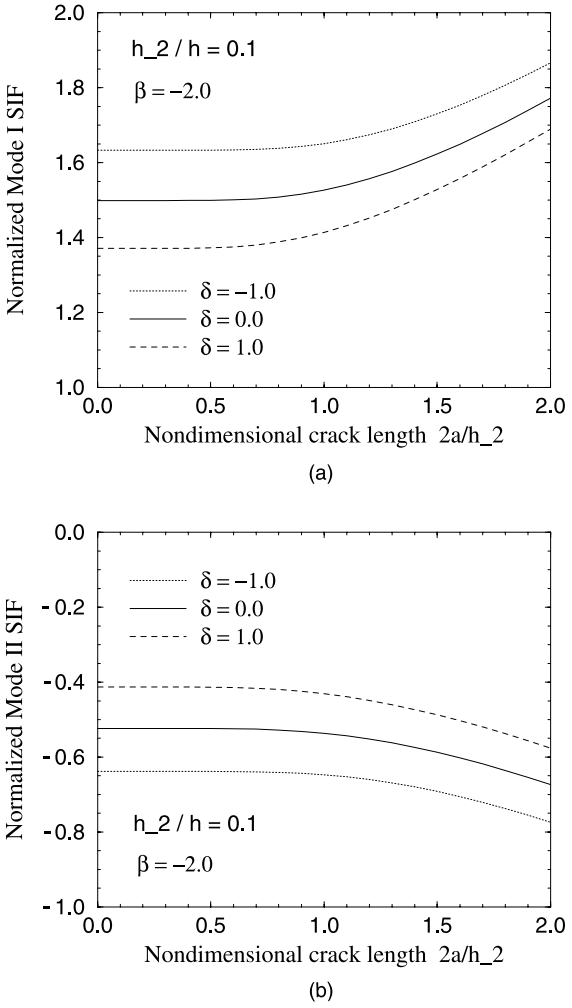

Fig. 8. Normalized SIFs versus nondimensional crack length, $2a/h_2$, for various material nonhomogeneous parameter δ considering the power law material with position-dependent relaxation time ($\beta = -2.0$, $h_2 = 0.1h$), (a) mode I SIF; (b) mode II SIF.

Appendix A

The Fredholm kernels $k_{ij}\ (r,s,\beta)$ $(i,j=1,2)$ in the system of integral equations (40) are given below [35]:

$$k_{11}(r,s,\beta) = \int_0^\infty [1 + 4\xi f_{11}(\xi)]\sin(r-s)\xi\,\mathrm{d}\xi,$$

$$k_{12}(r,s,\beta) = \int_0^\infty 4\xi f_{12}(\xi)\cos(r-s)\xi\,\mathrm{d}\xi,$$

$$k_{21}(r,s,\beta) = -\int_0^\infty 4\xi^2 f_{21}(\xi)\cos(r-s)\xi\,\mathrm{d}\xi,$$

$$k_{22}(r,s,\beta) = \int_0^\infty [1 + 4\xi^2 f_{22}(\xi)]\sin(r-s)\xi\,\mathrm{d}\xi.$$

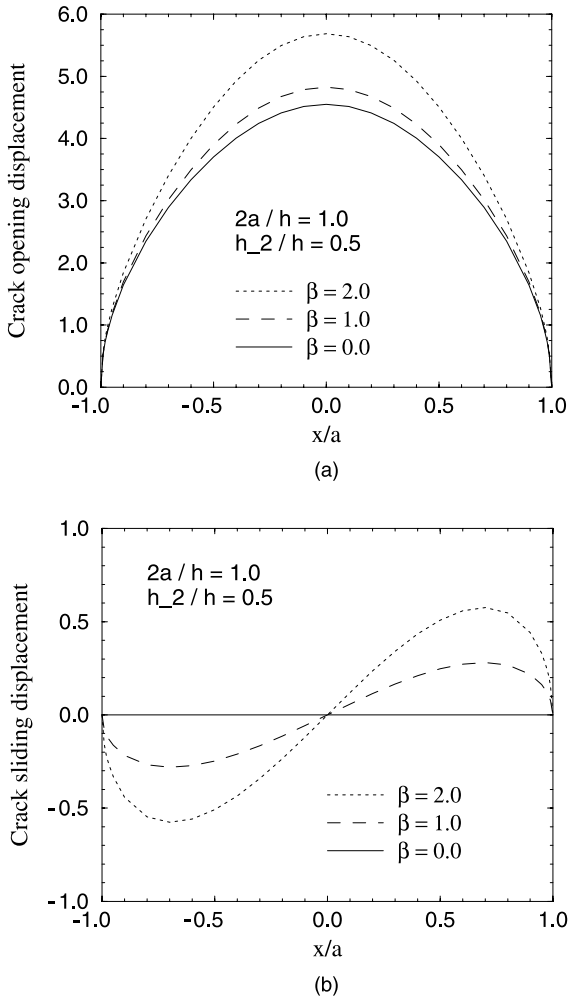

Fig. 9. Crack opening/sliding displacements for three β values, standard linear solid and power law material with constant relaxation time ($h_2 = 0.5h$, $2a/h = 1.0$), (a) mode I case; (b) mode II case.

The functions $f_{ij}(\xi)$ $(i, j = 1, 2)$ in the above equations are given by

$$f_{11}(\xi) = [-\beta H_{11} + s_2(s_1 - s_2)H_{12}]/(s_1 - s_2)^3,$$
$$f_{12}(\xi) = [-2\xi H_{11} - \xi(s_1 - s_2)H_{12}]/(s_1 - s_2)^3,$$
$$f_{21}(\xi) = [-\beta H_{21} + s_2(s_1 - s_2)H_{22}]/(s_1 - s_2)^3,$$
$$f_{22}(\xi) = [-2\xi H_{21} - \xi(s_1 - s_2)H_{22}]/(s_1 - s_2)^3,$$

in which

$$s_1 = -s - \beta/2, \quad s_2 = s - \beta/2, \quad s = \sqrt{\xi^2 + \beta^2/4},$$

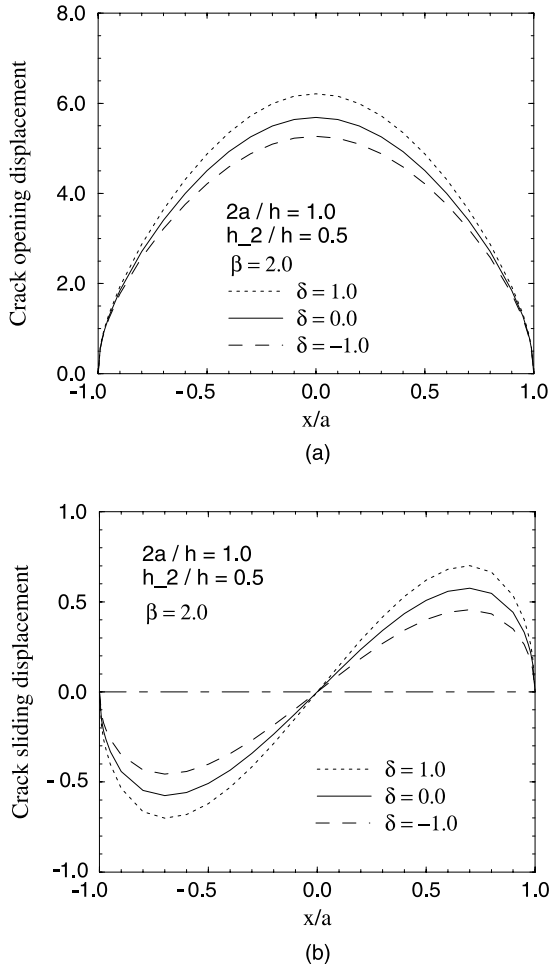

Fig. 10. Crack opening/sliding displacements for three δ values, power law material with position dependent relaxation time ($\beta = 2.0$, $h_2 = 0.5h$, $2a/h = 1.0$), (a) mode I case; (b) mode II case.

and

$$H_{11}(\xi) = (h_{11}d_{11} + h_{12}d_{21})/D_A,$$
$$H_{12}(\xi) = (h_{11}d_{12} + h_{12}d_{22})/D_A,$$
$$H_{21}(\xi) = (h_{21}d_{11} + h_{22}d_{21})/D_A,$$
$$H_{12}(\xi) = (h_{21}d_{12} + h_{22}d_{22})/D_A.$$

In the above expressions, the functions $h_{ij}(\xi)$ $(i, j = 1, 2)$ are given by

$$h_{11}(\xi) = -s_1 + \exp(-2sh_1)(s_1 + 2h_1 s s_2),$$
$$h_{12}(\xi) = 1 - \exp(-2sh_1)[1 - 2h_1 s(1 - h_1 s_2)],$$
$$h_{21}(\xi) = 1 - \exp(-2sh_1)(1 + 2sh_1),$$
$$h_{22}(\xi) = 2h_1^2 s \exp(-2sh_1),$$

the functions $d_{ij}(\xi)$ $(i,j=1,2)$ are

$$\begin{aligned}
d_{11}(\xi) &= \exp(-2hs)[1-2sh(1-2h_1s)-(1-2h_1s+4h_1^2s^2)+\exp(-2sh_2)] \\
&\quad +\exp(-2sh_2)(1+2h_2s+4h_2^2s^2)-1, \\
d_{12}(\xi) &= 2s\exp(-2hs)[h(h_1-h_2-2h_1h_2s)-h_1^2\exp(-2sh_2)]+2h_2^2s\exp(-2sh_2), \\
d_{21}(\xi) &= 4s^2\exp(-2hs)[h-h_1\exp(-2sh_2)]-4h_2^2s\exp(-2sh_2), \\
d_{22}(\xi) &= \exp(-2hs)[(1+2h_1s)(1+2h_2s-\exp(-2sh_2)+4h_2^2s^2)]+(1-2h_2s)\exp(-2sh_2)-1,
\end{aligned}$$

and $D_A(\xi)$ is

$$D_A(\xi) = 1-2(1+2h^2s^2)\exp(-2hs)+\exp(-4hs).$$

References

[1] Christensen RM. Theory of Viscoelasticity. New York: Academic Press; 1971.
[2] Broberg KB. Cracks and Fracture. London: Academic Press; 1999.
[3] Atkinson C, Chen CY. The influence of layer thickness on the stress intensity factor of a crack lying in an elastic (viscoelastic) layer embedded in a different elastic (viscoelastic) medium (mode III analysis). Int J Eng Sci 1996;34:639–58.
[4] Atkinson C, Chen CY. The influence of layer thickness on the stress intensity factor of a crack lying in an (visco)elastic layer embedded in a different (visco)elastic medium (plane strain, mode I analysis). Proc Royal Soc London: A 1997;453:1445–71.
[5] Knauss WG. The mechanics of polymer fracture. Appl Mech Rev 1973;26:1–17.
[6] Shapery RA. A theory of crack initiation and growth in viscoelastic media, I. Theoretical development. Int J Fract 1975;11:141–58.
[7] Shapery RA. A theory of crack initiation and growth in viscoelastic media, II. Approximate methods of analysis. Int J Fract 1975;11:549–62.
[8] Shapery RA. A theory of crack initiation and growth in viscoelastic media, III. Analysis of continuous growth. Int J Fract 1975;11:141–58.
[9] Hirai T. Functionally gradient materials. In: Brook RJ, editor. Materials Science and Technology, Processing of Ceramics, Part 2, vol. 17B. Weinheim, Germany: VCH Verlagsgesellschaft mbH; 1996. p. 292–341.
[10] Suresh S, Mortensen A. Functionally Graded Materials. London: The Institute of Materials, IOM Communications Ltd; 1998.
[11] Koizumi M. The concept of FGMs. In: Holt JB, Koizumi M, Hirai T, Munir Z, editors. Functionally Graded Materials, 34. Ohio: American Ceramic Society; 1993. p. 3–10.
[12] Aboudi J, Pindera MJ, Arnold SM. Higher-order theory for functionally graded materials. Compos Part B: Eng 1999;30B: 777–832.
[13] Erdogan F. Fracture mechanics of functionally graded materials. Compos Eng 1995;5:753–70.
[14] Eischen JW. Fracture of nonhomogeneous materials. Int J Fract 1987;34:3–22.
[15] Jin Z-H, Noda N. Crack-tip singular fields in nonhomogeneous materials. ASME J Appl Mech 1994;61:738–40.
[16] Jin Z-H, Batra RC. Some basic fracture mechanics concepts in functionally graded materials. J Mech Phys Solids 1996;44: 1221–35.
[17] Gu P, Asaro RJ. Crack deflection in functionally graded materials. Int J Solids Struct 1996;34:3085–98.
[18] Honein T, Herrmann G. Conservation laws in nonhomogeneous plane elastostatics. J Mech Phys Solids 1997;45:789–805.
[19] Paulino GH, Fannjiang AC, Chan YS. Gradient elasticity theory for a mode III crack in a functionally graded material. Mater Sci Forum 1999;308–311:971–6.
[20] Carpenter RD, Paulino GH, Munir ZA, Gibeling JC. A novel technique to generate sharp cracks in metallic/ceramic functionally graded materials by reverse 4-point bending. Scripta Materialia 2000;43:547–52.
[21] Becker Jr. TL, Cannon RM, Ritchie RO. A statistical RKR fracture model for the brittle fracture of functionally graded materials. Mater Sci Forum 1999;308–311:957–62.
[22] Parameswaran V, Shukla A. Dynamic fracture of functionally gradient material having discrete property variation. J Mater Sci 1998;33:3303–11.
[23] Lambros J, Santare MH, Li H, Sapna III GH. A novel technique for the fabrication of laboratory scale model functionally graded materials. Exp Mech 1999;39:184–90.

[24] Marur PR, Tippur HV. Dynamic response of bimaterial and graded interface cracks under impact loading. Int J Fract 2000;103:95–109.
[25] Paulino GH, Jin Z-H. Correspondence principle in viscoelastic functionally graded materials. ASME J Appl Mech 2001;68: 129–32.
[26] Paulino GH, Jin Z-H. Viscoelastic functionally graded materials subjected to antiplane shear fracture. ASME J Appl Mech 2001;68:284–93.
[27] Paulino GH, Jin Z-H. A crack in a viscoelastic functionally graded material layer embedded between two dissimilar homogeneous viscoelastic layers—antiplane shear analysis. Int J Fract 2001;111:283–303.
[28] Alex R, Schovanec L. An anti-plane crack in a nonhomogeneous viscoelastic body. Eng Fract Mech 1996;55:727–35.
[29] Herrmann JM, Schovanec L. Quasi-static mode III fracture in a nonhomogeneous viscoelastic body. Acta Mechanica 1990;85:235–49.
[30] Herrmann JM, Schovanec L. Dynamic steady-state mode III fracture in a nonhomogeneous viscoelastic body. Acta Mechanica 1994;106:41–54.
[31] Schovanec L, Walton JR. The quasi-static propagation of a plane strain crack in a power-law inhomogeneous linearly viscoelastic body. Acta Mechanica 1987;67:61–77.
[32] Schovanec L, Walton JR. The energy release rate for a quasi-static mode I crack in a nonhomogeneous linearly viscoelastic body. Eng Fract Mech 1987;28:445–54.
[33] Yang YY. Time-dependent stress analysis in functionally graded materials. Int J Solids Struct 2000;37:7593–608.
[34] Delale F, Erdogan F. On the mechanical modeling of the interfacial region in bonded half planes. ASME J Appl Mech 1988;55:317–24.
[35] Noda N, Jin Z-H. Thermal stress intensity factors for a crack in a strip of a functionally gradient material. Int J Solids Struct 1993;30:1039–56.
[36] Fung YC. Foundations of Solid Mechanics. Englewood Cliffs, NJ: Prentice Hall; 1965.
[37] Ogorkiewicz RM. Engineering Properties of Thermoplastics. London: Wiley-Interscience; 1970.
[38] Erdogan F, Gupta GD, Cook TS. Numerical solution of singular integral equations. In: Sih GC, editor. Mechanics of Fracture, vol. 1. Leyden: Noordhoff; 1973. p. 368–425.
[39] Tada H, Paris P, Irwin G. The Stress Analysis of Cracks Handbook. Hellertown, PA, USA: Del Research Corporation; 1973.
[40] Wnuk MP. Subcritical growth of fracture (inelastic fatigue). Int J Fract Mech 1971;7:383–407.